Theoretical Notes

Note 286

August 1976

Analytic Calculations of the Electromagnetic Fields From a Highly Space-Charge-Limited SGEMP Boundary Layer

by

Daniel F. Higgins
Mission Research Corporation
Santa Barbara, California 93102

Abstract

Analytic estimates of time-domain electromagnetic fields produced by a highly space-charge-limited SGEMP boundary layer are made using a dipole source current distribution. Near-zone and radiation-zone field terms are explicitly separated to show the importance of current density rise time and pulse width on the resulting EM waveforms. Both point sources and extended source regions are considered.

CONTENTS

ILLUSTRATIONS

SECTION 1

INTRODUCTION

In high fluence SGEMP situations[1,2] a thin, highly space-charge-limited boundary layer may be created near emitting surfaces. In many particle-following SGEMP codes, the presence of the boundary layer creates the necessity for very finely gridding up space near the emission surface. This small spatial grid can cause code running times to be excessively long or create problems in properly gridding up the rest of the system under consideration.

Proper treatment of this boundary layer is important not only for obtaining realistic electron trajectories but also for calculating correct electromagnetic fields. The thin boundary layer may be relatively inefficient (compared to electrons escaping to infinity) in creating satellite replacement currents, but, in high-fluence cases, the total amount of charge in the boundary layer may greatly exceed the charge that escapes.

It is thus useful to have some basic understanding of the electromagnetic fields from such a boundary layer. This report describes an analytic method for calculating such fields from known current and charge densities.

SECTION 2

ELECTROMAGNETIC FIELDS FROM A KNOWN SOURCE DISTRIBUTION

Maxwell's equations can be combined into the two vector wave equations

$$\nabla^2\vec{E} - \varepsilon\mu \frac{\partial^2 E}{\partial t^2} = \mu \frac{\partial \vec{J}}{\partial t} + \frac{1}{\varepsilon} \nabla\rho \ , \tag{1}$$

and

$$\nabla^2 H - \varepsilon\mu \frac{\partial^2 \vec{H}}{\partial t^2} = - \nabla \times \vec{J} \ . \tag{2}$$

The solution for $\vec{E}$ and $\vec{H}$ can be written as the integral equations

$$\vec{E}(\vec{r},t) = - \frac{1}{4\pi} \int \frac{[\mu \frac{\partial \vec{J}}{\partial t} + \frac{1}{\varepsilon} \nabla\rho]}{|\vec{r} - \vec{r}'|} \, d^3\vec{r}' \ , \tag{3}$$

and

$$\vec{H}(\vec{r},t) = - \frac{1}{4\pi} \int \frac{[-\nabla \times \vec{J}]}{|\vec{r} - \vec{r}'|} \, d^3\vec{r}' \ , \tag{4}$$

where the integral is over the source region specified by $\vec{r}'$ and the integrands are evaluated at the retarded time t' where

$$t' = t - \frac{|\vec{r} - \vec{r}'|}{c} \ . \tag{5}$$

Equations 3 and 4 can be written in a variety of other forms by integrating by parts, taking care to properly treat the retarded time dependence.

One form is just

$$\vec{E}(\vec{r},t) = -\frac{1}{4\pi\varepsilon}\nabla\int\frac{\rho(\vec{r}',t')}{|\vec{r}-\vec{r}'|}\,d^3\vec{r}' - \frac{\mu}{4\pi}\frac{\partial}{\partial t}\int\frac{\vec{J}(\vec{r}',t')}{|\vec{r}-\vec{r}'|}\,d^3\vec{r}' \quad , \tag{6}$$

and

$$\vec{H}(\vec{r},t) = \frac{1}{4\pi}\nabla\times\int\frac{\vec{J}(\vec{r}',t')}{|\vec{r}-\vec{r}'|}\,d^3\vec{r}' \quad . \tag{7}$$

These equations just agree with field expressions in terms of the vector potential, $\vec{A}$, and scalar potential, ϕ, where

$$\vec{H}(\vec{r},t) = \frac{1}{\mu}\nabla\times\vec{A} \quad , \tag{8}$$

$$\vec{E}(\vec{r},t) = -\nabla\phi - \frac{\partial\vec{A}}{\partial t} \quad , \tag{9}$$

and

$$\phi(\vec{r},t) = \frac{1}{4\pi\varepsilon}\int\frac{\rho(\vec{r}',t')}{|\vec{r}-\vec{r}'|}\,d^3\vec{r}' \quad , \tag{10}$$

$$\vec{A}(\vec{r},t) = \frac{\mu}{4\pi}\int\frac{\vec{J}(\vec{r}',t')}{|\vec{r}-\vec{r}'|}\,d^3\vec{r}' \quad . \tag{11}$$

Equations 6 and 7 can be further transformed to the forms

$$\vec{E}(\vec{r},t) = \frac{1}{4\pi}\int\left\{\frac{1}{\varepsilon}\left[\rho(\vec{r}',t') + \frac{|\vec{r}-\vec{r}'|}{c}\,\frac{\partial\rho}{\partial t'}(\vec{r}',t')\right]\frac{(\vec{r}-\vec{r}')}{|\vec{r}-\vec{r}'|^3} - \frac{\mu}{|\vec{r}-\vec{r}'|}\frac{\partial\vec{J}}{\partial t'}(\vec{r}',t')\right\}d^3\vec{r}' \quad , \tag{12}$$

and

$$\vec{H}(\vec{r},t) = \frac{1}{4\pi}\int \left[\vec{J}(\vec{r}',t') + \frac{|\vec{r}-\vec{r}'|}{c}\frac{\partial \vec{J}}{\partial t}(\vec{r}',t')\right] \times \frac{(\vec{r}-\vec{r}')}{|\vec{r}-\vec{r}'|^3}\, d^3\vec{r}' \,. \quad (13)$$

Equation 12 can be further transformed, using the charge continuity equation to obtain

$$\vec{E}(\vec{r},t) = \frac{1}{4\pi}\int \left\{\frac{1}{\varepsilon}\left[\frac{\rho(\vec{r}',t')}{|\vec{r}-\vec{r}'|^3}(\vec{r}-\vec{r}') - \frac{1}{c}\left[\vec{J}(\vec{r}',t')\cdot\nabla\right]\frac{(\vec{r}-\vec{r}')}{|\vec{r}-\vec{r}'|^2}\right]\right.$$

$$\left. + \frac{\mu}{|\vec{r}-\vec{r}'|}\,\frac{(\vec{r}-\vec{r}')}{|\vec{r}-\vec{r}'|} \times \left[\frac{(\vec{r}-\vec{r}')}{|\vec{r}-\vec{r}'|} \times \frac{\partial \vec{J}}{\partial t}(\vec{r}',t')\right]\right\} d^3\vec{r}' \,. \quad (14)$$

The forms of Equations 13 and 14 are convenient in that the radiation terms (i.e., the part of the field that falls off as $|\vec{r}|^{-1}$ as $|\vec{r}|$ goes to infinity) is readily identified. In each case, the radiated field depends upon $\partial\vec{J}/\partial t$, since the contributions of the other source terms fall off faster than $|\vec{r}|^{-1}$.

SECTION 3

ELECTROMAGNETIC FIELDS FROM A POINT DIPOLE SOURCE

A. GENERAL FORMULAS

A reasonable starting point for calculating the EM fields from the SGEMP boundary layer is to consider the fields from a point dipole source. Such results should well represent the fields far from a finite size boundary layer region, and even nearby fields can then be written as a summation over the source region of point dipole fields. The solution for fields from a point dipole is thus a Green's function that can be used in further calculations.

For these calculations, let us assume that the observer is at the origin, O, of a Cartesian coordinate system and that the dipole is centered at $\vec{r}' = (x_1, y_1, 0)$. The dipole is then described by

$$\vec{J} = I\ \delta(x-x_1)\ \delta(y-y_1)\ \hat{z}, \qquad -a \le z \le a$$

$$= 0 \qquad \text{otherwise} \tag{15}$$

and

$$\rho = Q\ \delta(x-x_1)\ \delta(y-y_1)\ \delta(z-a)$$

$$- Q\ \delta(x-x_1)\ \delta(y-y_1)\ \delta(z+a) \tag{16}$$

Note that Q and I are arbitrary functions of time and it is also assumed that

$$I = \frac{dQ}{dt} \quad . \tag{17}$$

For the calculations it is also assumed that $Q = 0$ at $t = 0$.

Note also that this choice of $\vec{J}$ and ρ is equivalent to electron emission from one point of a perfectly conducting plane that coincides with the x-y plane. Currents and charges below the plane are just images of those above the plane. It is apparent from symmetry considerations that $\vec{E}$ and $\vec{H}$ have the proper values (i.e., the proper boundary conditions) to consider the xy-plane as a perfect conductor.

Now, from Equations 12 and 14, the electromagnetic fields can be written as

$$\vec{E}(\vec{r},t) = \frac{1}{4\pi}\int \left\{ \frac{1}{\varepsilon}\left[\rho(\vec{r}',t') + \frac{|\vec{r}-\vec{r}'|}{c}\ \frac{\partial\rho}{\partial t'}(\vec{r}',t')\right]\frac{(\vec{r}-\vec{r}')}{|\vec{r}-\vec{r}'|^3} - \frac{\mu}{|\vec{r}-\vec{r}'|}\ \frac{\partial\vec{J}}{\partial t'}(\vec{r}',t')\right\} d^3r' \tag{18}$$

and

$$\vec{H}(\vec{r},t) = \frac{1}{4\pi}\int \left[\vec{J}(\vec{r}',t') + \frac{|\vec{r}-\vec{r}'|}{c}\ \frac{\partial\vec{J}}{\partial t'}(\vec{r}',t)\right] \times \frac{\vec{r}-\vec{r}'}{|\vec{r}-\vec{r}'|^3} \tag{19}$$

For the case in question, these integrals are easily evaluated if one assumes that the dipole thickness, 2a, is small compared to other dimensions of interest. Then signals from all parts of the current filament will arrive at the observer at approximately the same retarded time, and one obtains

$$\vec{E}(0,t) = -\left[\frac{2a\ Q(t')}{4\pi\varepsilon_o\ R^3} + \frac{2a}{4\pi\varepsilon_0\ R^2 c}\ \frac{\partial Q(t')}{\partial t'} + \frac{\mu}{4\pi}\ \frac{2a}{R}\ \frac{\partial I(t')}{\partial t'}\right]\hat{z} \tag{20}$$

$$\vec{H}(0,t) = \frac{2a}{4\pi R}\left[\frac{I(t')}{R} + \frac{1}{c}\frac{\partial I(t')}{\partial t'}\right](\hat{z} \times \hat{n}) \qquad (21)$$

where

$$R = \sqrt{x_1^2 + y_1^2}$$

$\hat{z}$ = unit vector parallel to z-axis

and

$$\hat{n} = -\frac{(x_1\hat{x} + y_1\hat{y})}{R} = \text{unit vector along } -\vec{r}'$$

Note that the electric field, $\vec{E}$, is made up of three distinct terms: a static field, proportional to Q ($\int Idt'$); a quasi-static field, proportional to $\partial Q/\partial t'$ (I); and a radiation zone field, depending upon $\partial^2 Q/\partial t'^2$ ($\partial I/\partial t'$). Similarly, the magnetic field, $\vec{H}$, has a static part, depending upon I , and a radiated part, depending upon $\partial I/\partial t'$.

Note also that the electric field vector is parallel to the z-axis while the magnetic field vector is in the x-y plane. More exactly, the direction of the magnetic field vector is given by

$$\hat{z} \times \hat{n} = \frac{y_1}{R}\hat{x} - \frac{x_1}{R}\hat{y} \qquad (22)$$

B. FIELDS FOR A TRIANGULAR CURRENT TIME HISTORY

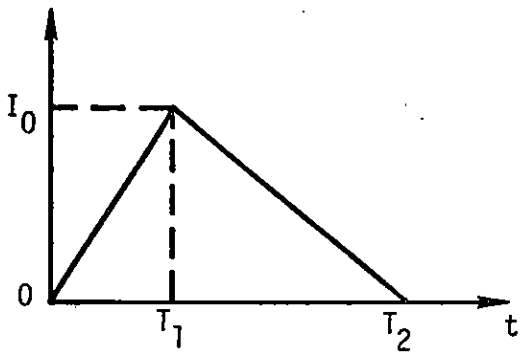

Figure 1. Triangular time history.

Let us assume that the current in the dipole follows the triangular time history shown in Figure 1. This time history is described by

$$I(t) = I_0\left(\frac{t}{T_1}\right), \qquad 0 \le t \le T_1$$

$$I(t) = I_0\left(1 - \frac{t-T_1}{T_2-T_1}\right), \qquad T_1 \le t \le T_2 \tag{23}$$

Equation 21 is then easily evaluated for $\vec{H}$ with the result that

$$|\vec{H}(0,t)| = \frac{2a}{4\pi}\,\frac{I_0}{R}\,\frac{1}{cT_1}\left[\frac{ct'}{R} + 1\right], \qquad 0 \le t' \le T_1$$

$$= \frac{2a}{4\pi}\,\frac{I_0}{R}\,\frac{1}{cT_1}\left\{\frac{T_1}{T_2-T_1}\left[\frac{c(T_2-t')}{R} - 1\right]\right\}, \qquad T_1 \le t' \le T_2 \tag{24}$$

where t' is the retarded time $t-R/c$. For $t' < 0$ (i.e., for $t < R/c$), the fields are zero.

Note that because the assumed triangular current time history has a discontinuous slope, the magnetic field waveform has several step-function discontinuities (at $t' = 0, T_1, T_2$). These step-function discontinuities correspond to the radiation zone field (which depends upon $\partial I/\partial t$).

Equation 20 can also be evaluated for the electric field, using

$$\frac{\partial Q}{t'} = I(t') \tag{25}$$

and

$$Q(t') = \int_0^{t'} I(t)dt \ . \tag{26}$$

From Equations 23 and 26

$$Q(t) = \frac{I_0 t^2}{2} \quad , \qquad 0 \le t \le T_1$$

$$= \frac{I_0}{T_2-T_1}\left\{-\frac{t^2}{2} + T_2 t - \frac{T_1T_2}{2}\right\} \ , \ T_1 \le t \le T_2 \tag{27}$$

The expression for the electric field thus becomes

$$\left|\vec{E}(0,t)\right| = \frac{\mu_0}{2\pi}\frac{a}{R}\frac{I_0}{T_1}\left\{\frac{c^2t'^2}{2R^2} + \frac{ct'}{R} + 1\right\} \quad , \tag{28a}$$

for $0 \le t \le T_1$

and

$$\left|\vec{E}(0,t)\right| = \frac{\mu_0}{2\pi}\frac{a}{R}\frac{I_0}{(T_2-T_1)}\left\{\frac{c^2}{R^2}\left[-\frac{t'^2}{2} + T_2t' - \frac{T_1T_2}{2}\right] + \frac{c}{R}[T_2-T'] - 1\right\} \tag{28b}$$

for $T_1 \le t \le T_2$

Note that these expressions imply that at the end of the current pulse (i.e., at $t' = T_2$) there exists some total charge, Q_T, at distance a above the x-y plane. This charge, which is given by

$$Q_T = \frac{I_0 T_2}{2} \quad , \tag{29}$$

just represents the total charge in space once the steady-state space-charge-limiting situation is set up. The electric field at $t' = T_2$ is thus just the static field from the electric dipole layer.

Waveforms for the electric and magnetic fields are shown in Figures 2-4, where the triangular time history was assumed to be symmetric with $T_1 = T$ and $T_2 = 2T_1 = 2T$. In these figures the normalized waveforms are plotted for several values of cT/R. Changing the value of this ratio can be thought of as varying either the pulse width (T) or the distance to the observer (R).

Note that there is a distinct change in waveform shape as cT/R increases. [Waveform magnitudes can not be directly compared since the normalization factor contains both R and T]. For $cT/R \lesssim 1$, the field waveform is bipolar and the step-function jumps are of primary importance in determining waveform shape. These values of cT/R correspond to the observer being in the radiation field zone. For large cT/R, on the other hand, the waveforms are more monopolar and the step-function jumps are less apparent. Thus, for $cT/R \gg 1$, the observer is in the near field zone.

It is also interesting to calculate the peak replacement current, I_p, that would flow if the x-y plane were perfectly conducting. In this case, the peak magnetic field at position 0 is numerically equal to the peak skin current density at that point. The peak current is then just

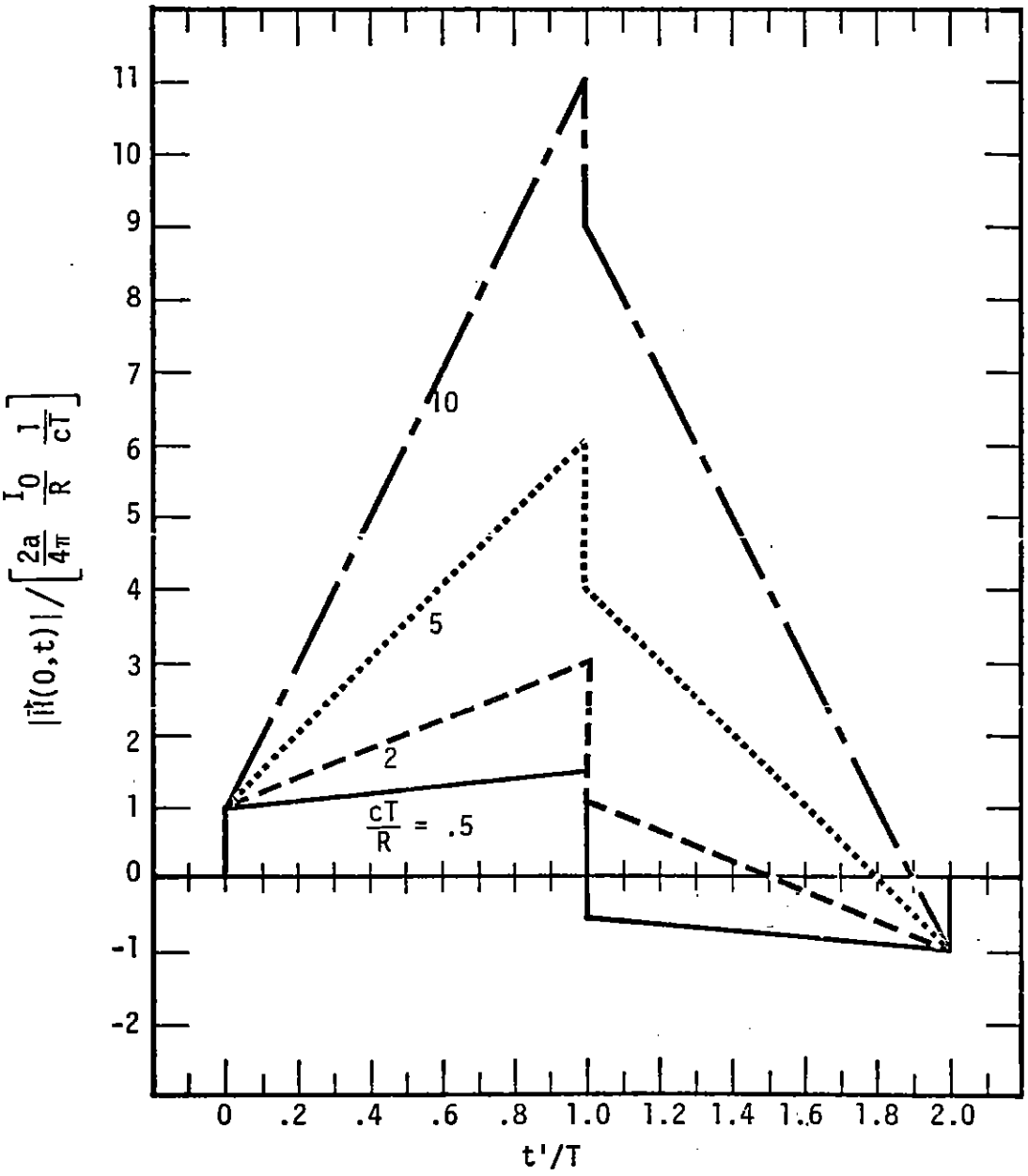

Figure 2. Magnetic field for a triangular current time history ($T_2 = 2T_1 = T$) with cT/R as a parameter.

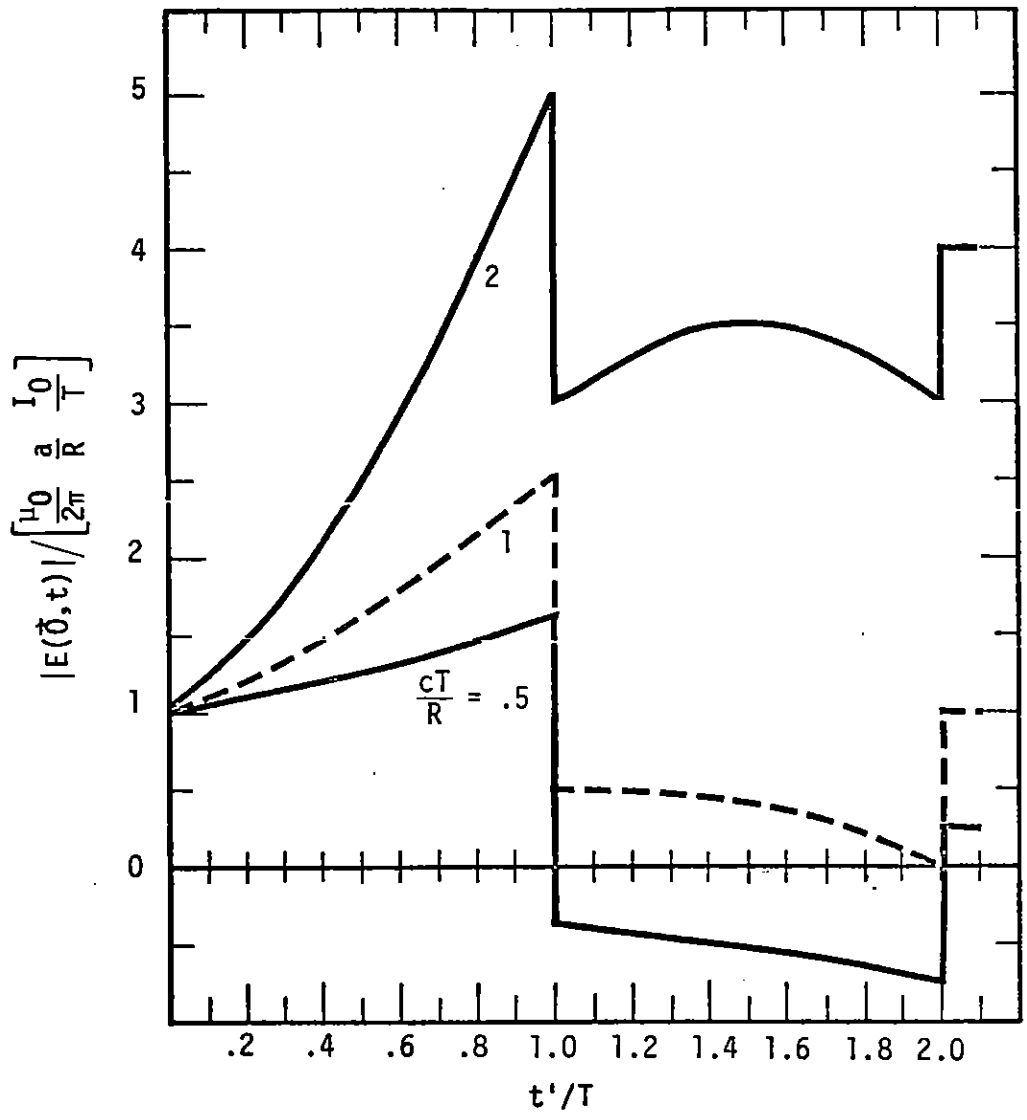

Figure 3. Electric field for a triangular current time history ($T_2 = 2T_1 = T$) with cT/R as a parameter (cT/R small).

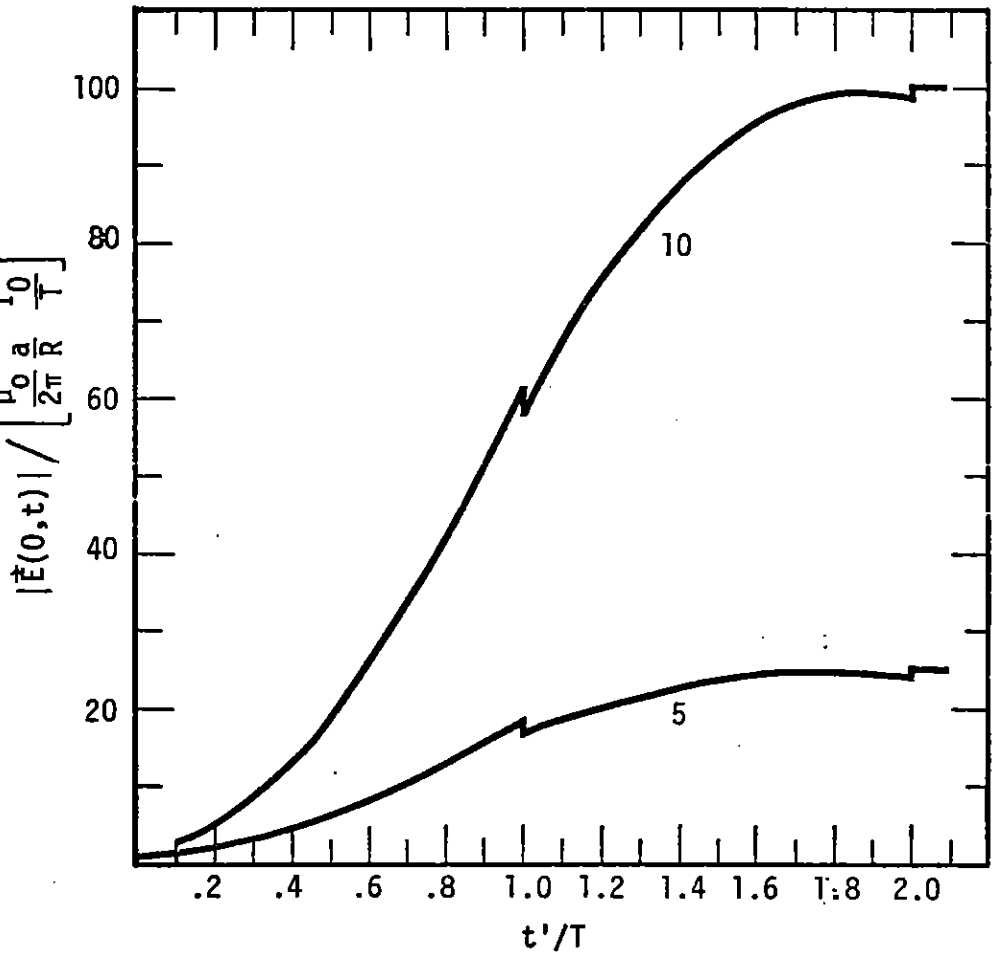

Figure 4. Electric field for a triangular current time history ($T_2 = 2T_1 = T$) with cT/R as a parameter (cT/R large).

$2\pi R$ times the peak magnetic field. From Equation 24, the peak magnetic field occurs at $t' = T_1$, so that

$$I_P = I_0 \left(\frac{a}{cT_1}\right)\left[\frac{cT_1}{R} + 1\right] \tag{30}$$

Far from the source, cT_1/R is small and the replacement current is just a constant fraction of the emission current. For short pulses and nearby observers, $cT/R \gg 1$ and the peak replacement current decreases linearly with R.

C. FIELDS FROM A SINE-SQUARED CURRENT TIME HISTORY

A somewhat more realistic time history for the current in the dipole layer can be defined by the expression

$$I(t) = I_0 \sin^2 \left(\frac{t}{2T} \pi\right) \tag{31}$$

This time history is shown in Figure 5. It has the advantage over a triangular time history of having continuous derivatives, a property more representative of any physical current.

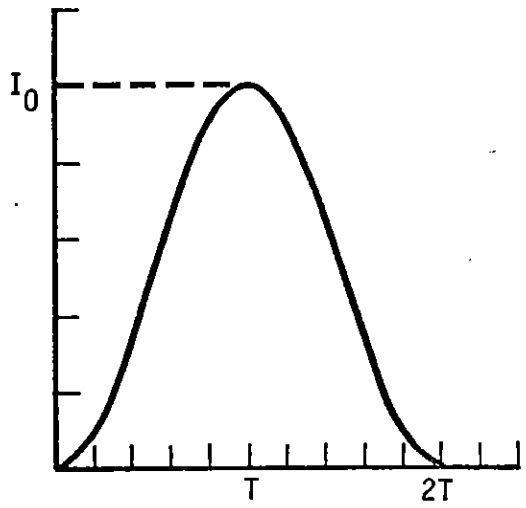

Figure 5. Sine-squared time history.

Equation 21 can then be evaluated for the magnetic field, using Equation 31, with the result that

$$|\vec{H}(0,t)| = \frac{2a}{4\pi}\frac{I_0}{R}\frac{1}{cT}\left[\frac{cT}{R}\sin^2\left(\frac{t'}{2T}\pi\right)\right.$$

$$\left. + \pi \sin\left(\frac{t'}{2T}\pi\right)\cos\left(\frac{t'}{2T}\pi\right)\right], \quad 0 \le t' \le 2T \tag{32}$$

In this case, the magnetic field waveform does not have any step-function discontinuities. Note also that the radiation zone fields come from the second term inside the parenthesis. The radiation field will be larger than the near-zone field whenever this second term is larger than the first term; i.e., when

$$\frac{cT}{\pi R}\tan\left(\frac{t'}{2T}\pi\right) < 1 \tag{33}$$

For this case the integral of the current gives a charge of

$$Q(t') = \frac{I_0 T}{\pi}\left[\frac{\pi t'}{2T} - \sin\left(\frac{t'}{2T}\pi\right)\cos\left(\frac{t'}{2T}\pi\right)\right] \tag{34}$$

so that Equation 20 can be evaluated for the electric field with the result that

$$|\vec{E}(0,t)| = \frac{\mu_0}{2\pi}\frac{a}{R}\frac{I_0}{T}\left\{\frac{c^2T^2}{R^2}\left[\frac{t'}{2T} - \frac{\sin\left(\frac{t'}{2T}\pi\right)\cos\left(\frac{t'}{2T}\pi\right)}{\pi}\right]\right.$$

$$\left. + \frac{cT}{R}\sin^2\left(\frac{t'}{2T}\pi\right) + \pi \sin\left(\frac{t'}{2T}\pi\right)\cos\left(\frac{t'}{2T}\pi\right)\right\} \tag{35}$$

Electric and magnetic field waveforms for this time history are plotted in Figures 6-8, using the same normalization factors as were used for the triangular time history. A comparison of these waveforms with those for the triangular time history in Figures 2-4 shows that the waveforms for

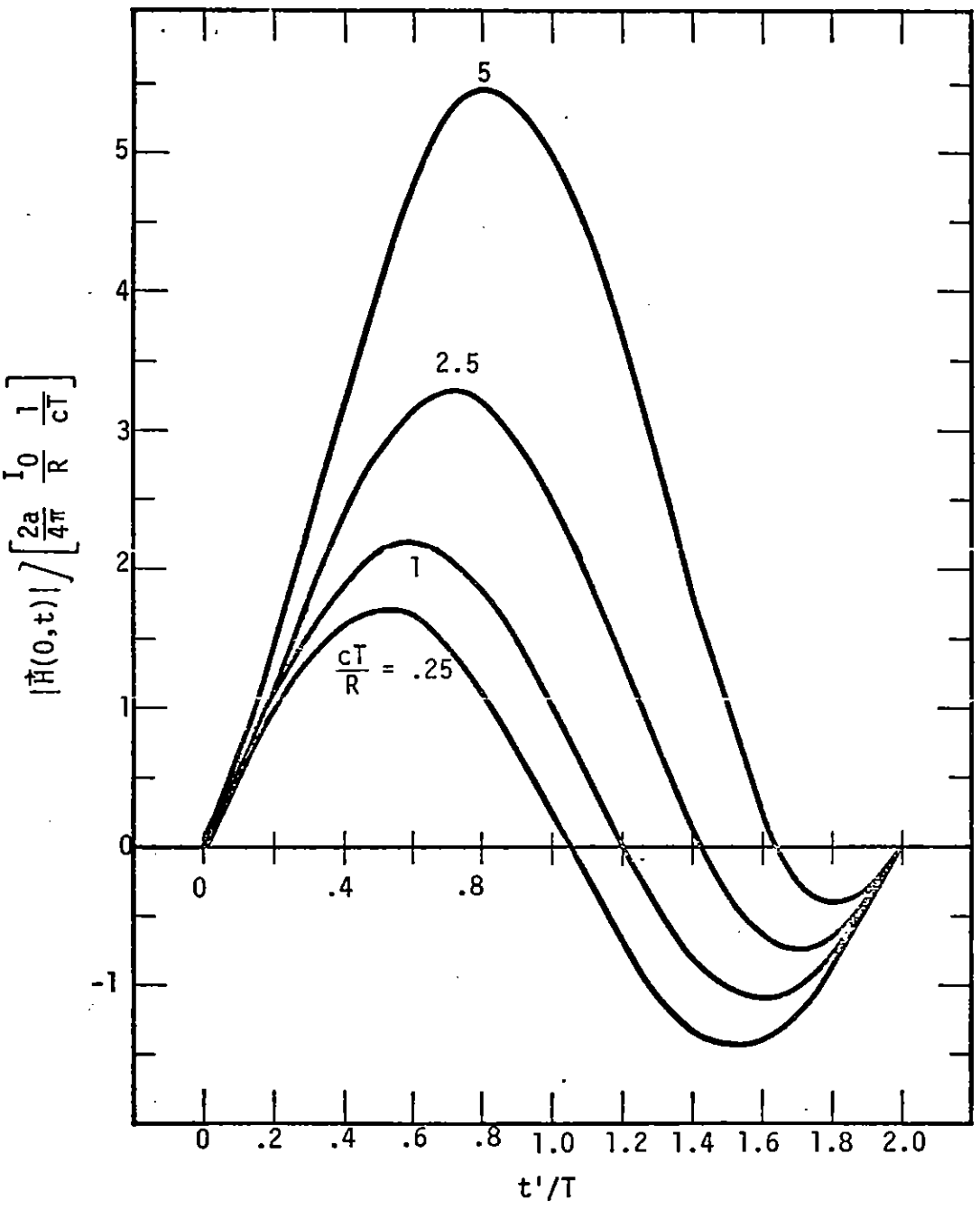

Figure 6. Magnetic field for a sine-squared current time history with cT/R as a parameter.

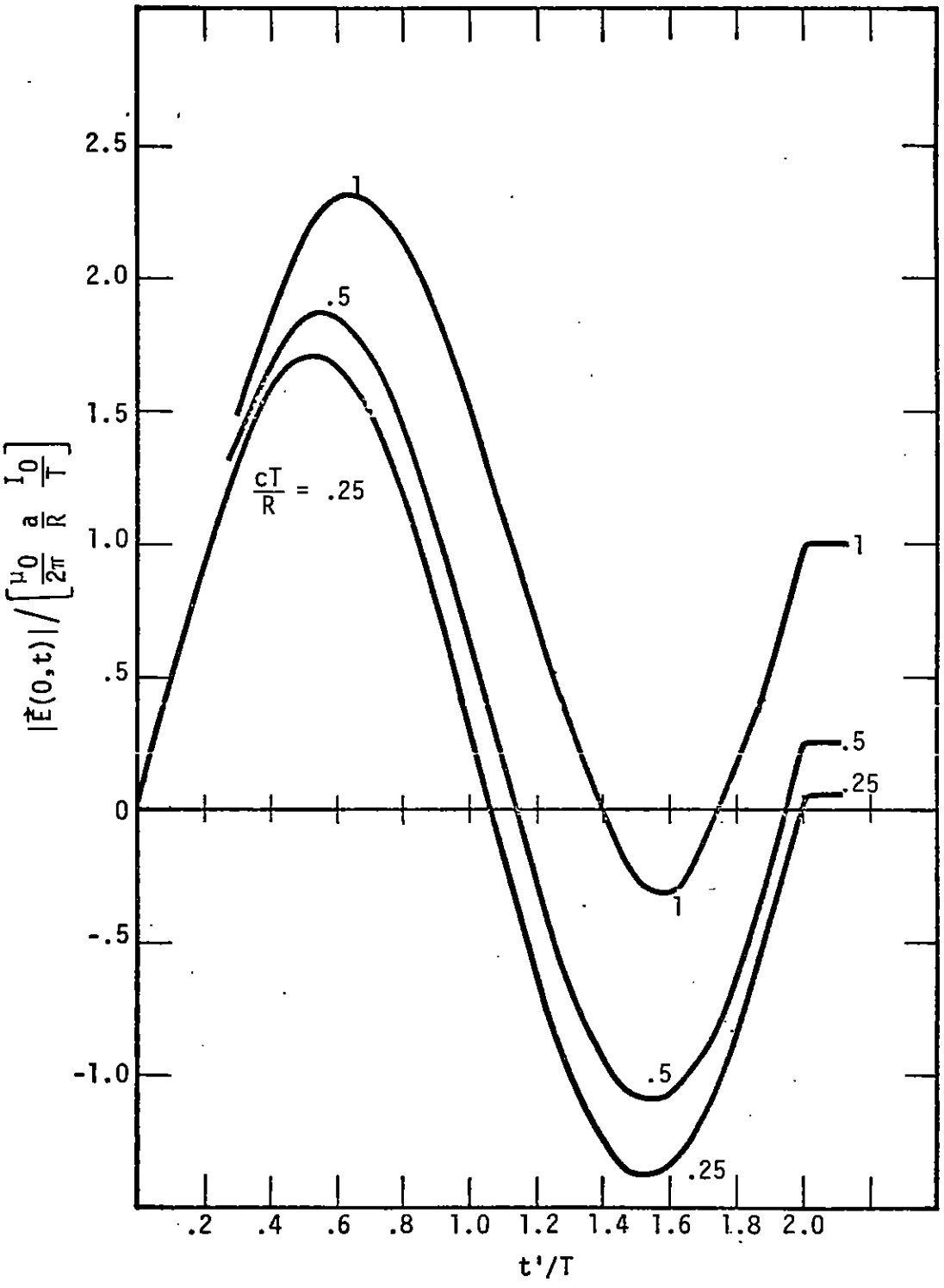

Figure 7. Electric field for a sine-squared current time history with cT/R as a parameter (small cT/R).

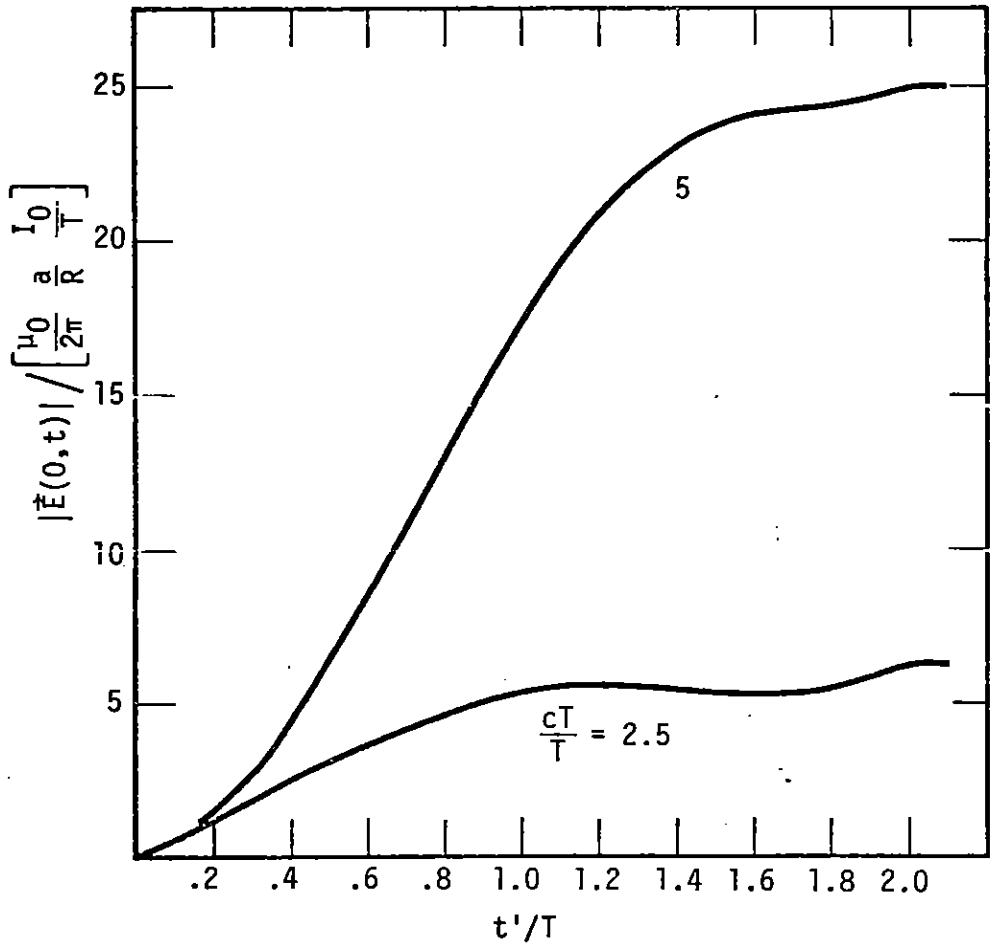

Figure 8. Electric field for a sin-squared current time history with cT/R as a parameter (large cT/R).

equal cT/R values are quite similar. This indicates the step-function jumps in the triangular time history waveforms simply become steep gradients when more realistic time histories are assumed.

SECTION 4

FIELDS FROM EXTENDED SOURCE REGIONS

A. INTRODUCTION

In the previous section of this report the electromagnetic fields from point sources were calculated for several assumed time histories. In this section, the fields from extended source regions will be considered. The fact that the SGEMP emission region is not a point source is, of course, most important for an observer near the region. Finite size source regions can be treated by simply combining the fields from each small section of the region with the proper time delay to account for retardation. In this section we will continue to assume that the source region is thin (i.e., a is small compared to other dimensions of interest). Also, for simplicity, we will consider only the linearly rising part of a triangular time history.

First consider a half-plane source region as shown in Figure 9 where the region defined by $x \geq D$, $-a \leq z \leq a$ contains a uniform current density directed in the z-direction. If J_0 is the peak current density, then the total peak current from each element of area, dA, is just

$$I_0 = J_0 dA \ , \tag{36}$$

and, from Equations 21 and 24 the magnetic field at the origin (point 0) is just given by

$$H_y = - \frac{2a}{4\pi} \frac{J_0}{cT_1} \iint \frac{\left[1 + \frac{ct'}{R}\right]}{R^2} \ x_1 \ dx_1 dy_1 \ . \tag{37}$$

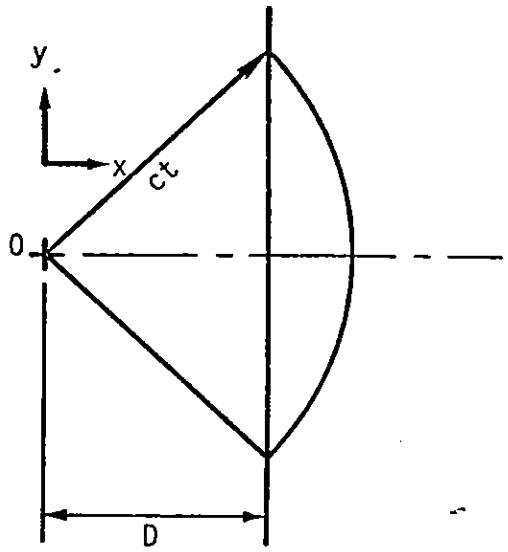

Figure 9. Geometry for half-plane emission.

(Note that from symmetry considerations, H_x is obviously equal to zero.) The above expression just sums the contributions from each small area of the half-plane, assuming that the current density is linearly rising with a slope equal to J_0/T_1.

Because of the retarded time term in the integrand, one must be careful in choosing the limits of the double integral in Equation 37. Remembering that

$$ct' = ct - R \ , \tag{38}$$

one can reduce the expression for H_y to

$$H_y = - \frac{a}{2\pi} J_0\left(\frac{t}{T_1}\right) \iint \frac{x_1}{(x_1^2+y_1^2)^{3/2}} \ dx_1 \ dy_1 \ , \tag{39}$$

where one must remember that H_y is zero for $t < D/c$. The integration over y_1 then extends from $-y_{max}$ to $+y_{max}$ where y_{max} is determined

by the limits of a circle of radius ct; i.e., for a given x_1,

$$x_1^2 + y_{max}^2 = ct \ , \tag{40}$$

or

$$y_{max} = \sqrt{c^2t^2 - x_1} \ . \tag{41}$$

The expression for H_y then becomes

$$H_y = -\frac{a}{\pi} J_0\left(\frac{t}{T_1}\right) \int_{x_{min}}^{x_{max}} \frac{y_{max}}{x_1\sqrt{x_1^2+y_{max}^2}} \, dx_1$$

$$= -\frac{a}{\pi} J_0\left(\frac{t}{T_1}\right) \int_{D}^{ct} \frac{\sqrt{c^2t^2-x_1^2}}{ct \ x_1} \, dx_1$$

$$= \frac{a}{\pi} J_0\left(\frac{t}{T_1}\right) \left[\sqrt{1 - \frac{D^2}{c^2t^2}} - \ln\left|\frac{1 + \sqrt{1 - D^2/c^2t^2}}{D/ct}\right|\right], \tag{42}$$

for $t \geq D/c$.

It is sometimes convenient to write H_y in terms of the time t_r, which is measured from the moment when the observer first "sees" the half-plane; i.e.,

$$t_r = t - D/c \ . \tag{43}$$

Equation 42 can then be rewritten as

$$H_y = \frac{a}{\pi} J_0 \frac{(ct_r+D)}{cT_1} \left[\frac{\sqrt{(1+\frac{ct_r}{D})^2 - 1}}{1 + \frac{ct_r}{D}} - \ln\left|1 + \frac{ct_r}{D} + \sqrt{(1+\frac{ct_r}{D})^2 - 1}\right|\right] . \tag{44}$$

B. RECTANGULAR SOURCE REGION

Now consider the rectangular source region shown in Figure 10. Note that for $ct \le \sqrt{D^2 + h^2/4}$, the rectangular region will give the same fields as a half-plane, since the observer at 0 will "see" only the edge of the rectangular region. The integrals also simplify when $ct \ge \sqrt{(D+b)^2 + h^2/4}$, since the observer will then "see" all of source region. For this case, $y_{max} = h/2$ and

$$H_y = -\frac{a}{\pi} J_0\left(\frac{t}{T_1}\right) \frac{h}{2} \int_{x=D}^{D+b} \frac{dx_1}{x_1 \sqrt{x_1^2 + h^2/4}}$$

$$= \frac{a}{\pi} J_0\left(\frac{t}{T_1}\right) \ell n \left| \left(\frac{1}{1 + \frac{b}{D}} \right) \left(\frac{\frac{h}{2D} + \sqrt{(1 + \frac{b}{D})^2 + (\frac{h}{2D})^2}}{\frac{h}{2D} + \sqrt{1 + (\frac{h}{2D})^2}} \right) \right| . \qquad (45)$$

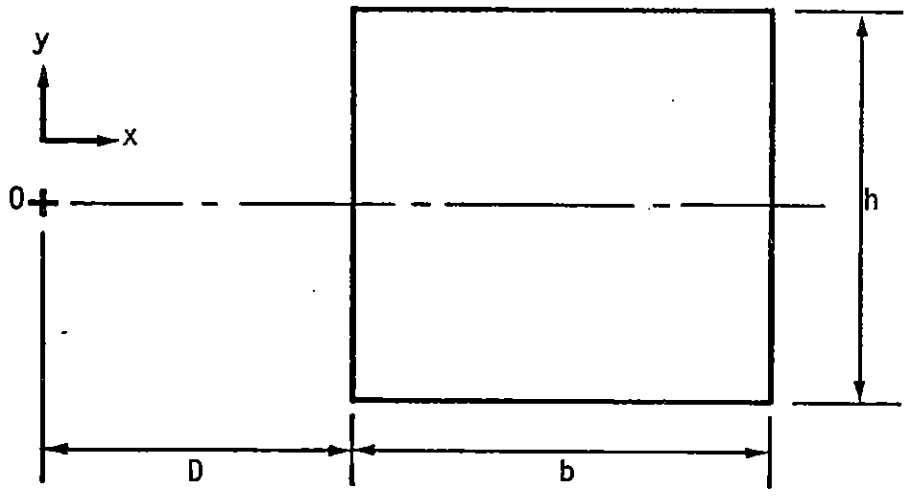

Figure 10. Geometry for rectangular source region.

Note that for a distant observer, D >> b,h, and

$$\lim_{\frac{b}{D},\,\frac{h}{D}\to 0}\left[\ln\left|\left(\frac{1}{1+\frac{b}{D}}\right)\left(\frac{\frac{h}{2D}+\sqrt{(1+\frac{b}{D})^2+(\frac{h}{2D})^2}}{\frac{h}{2D}+\sqrt{1+(\frac{h}{2D})^2}}\right)\right|\right]=-\frac{bh}{2D^2}\,. \quad (46)$$

This implies that

$$\lim_{\frac{b}{D},\,\frac{h}{D}\to 0}[H_y]=-\frac{2a}{4\pi}\frac{I_0}{D}\frac{1}{cT_1}\left[\frac{ct_r}{D}+1\right]\,, \quad (47)$$

where $I_0 = J_0 bh$ and t_r was defined in Equation 43. Note that in the limit of large D, retarded times for all source points in the rectangular source region are approximately equal, so that t_r is just the "average" retarded time. Equation 47 is then equivalent to Equation 24, which gives the field for a point source region.

One can also calculate H_y for times in the range $\sqrt{D^2 + h^2/4} \le ct \le \sqrt{(D+b)^2 + h^2/4}$, but the expressions are a little more complex.

For times in this region, the field can be broken into several parts, corresponding to regions I and II of Figure 11.

The field from region I is just that of a rectangular source of dimensions d by h where

$$d = \sqrt{c^2t^2 - h^2/4} - D\,. \quad (48)$$

Thus

$$H_I = \frac{a}{\pi} J_0\left(\frac{t}{T_1}\right) \ln\left|\left(\frac{D}{D+d}\right)\left(\frac{h/2+\sqrt{(D+d)^2+h^2/4}}{h/2+\sqrt{D^2+h^2/4}}\right)\right|\,. \quad (49)$$

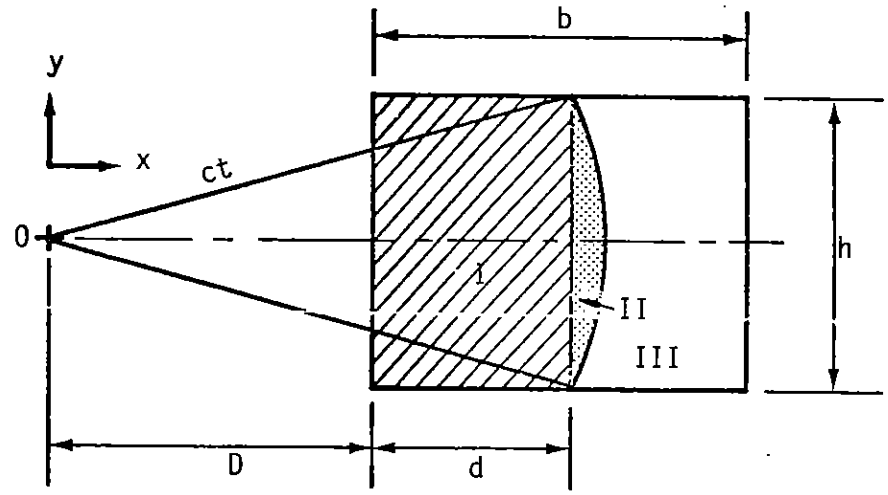

Figure 11. Parts of the source region for a rectangular source.

The field from region II is just that of a half-plane for $ct < D + d$ (i.e., before the observer can "see" the far edge of the source region). In more general terms, one can write

$$H_{II} = -\frac{a}{\pi} J_0\left(\frac{t}{T_1}\right)\left[\sqrt{1 - \frac{x^2}{c^2t^2}} - \ell n\left|\frac{1 + \sqrt{1 - \left(\frac{x}{ct}\right)^2}}{(x/ct)}\right|\right]\Bigg|_{x = d + D}^{x = Sm(ct,D+b)} \qquad (50)$$

where $Sm(ct, D+b)$ indicates that one uses the smaller of the two quantities inside the parenthesis as the upper limit.

The total field at point 0 is then just the sum of H_I and H_{II}.

For comparison with the point source case, it is convenient to express the magnetic field as

$$H_y = -\frac{a}{2\pi}\frac{(J_0 bh)}{D}\frac{1}{cT_1}\left(\frac{ct_r}{D}+1\right)\gamma \qquad (51)$$

so that γ is the ratio of finite size source region field to the field from a point source. As noted previously, the value of γ will depend upon how much of the source region can be "seen" by the observer.

For $0 \le \frac{ct_r}{D} \le \sqrt{1+\left(\frac{h}{2D}\right)^2} - 1$, the observer "sees" only the front edge of the source region and

$$\gamma = \left(-\frac{2D^2}{bh}\right)\left[\frac{\sqrt{\left(1+\frac{ct_r}{D}\right)^2 - 1}}{\left(1+\frac{ct_r}{D}\right)} - \ell n\left|1+\frac{ct_r}{D}+\sqrt{\left(1+\frac{ct_r}{D}\right)^2-1}\right|\right]. \qquad (52)$$

For $\sqrt{1+\left(\frac{h}{2D}\right)^2} - 1 \le \frac{ct_r}{D} \le \sqrt{\left(1+\frac{b}{D}\right)^2+\left(\frac{h}{2D}\right)^2} - 1$, the observer "sees" part, but not all, of the rectangular source region. Thus, in this time interval,

$$\gamma = \gamma_I + \gamma_{II}\ , \qquad (53)$$

where γ_I and γ_{II} refer to H_I and H_{II} as previously defined. Now,

$$\gamma_I = \left(-\frac{2D^2}{bh}\right)\ell n\left|\left(\frac{1}{1+\frac{d}{D}}\right)\left(\frac{\frac{h}{2D}+\sqrt{\left(1+\frac{d}{D}\right)^2+\left(\frac{h}{2D}\right)^2}}{\frac{h}{2D}+\sqrt{1+\left(\frac{h}{2D}\right)^2}}\right)\right|\ , \qquad (54)$$

where

$$\frac{d}{D} = \sqrt{\left(\frac{ct_r}{D}+1\right)^2 - \left(\frac{h}{2D}\right)^2} - 1\ . \qquad (55)$$

γ_{II} is simplified by further subdividing the time interval. For $\sqrt{1 + (h/2D)^2} - 1 \le ct_r/D \le b/D$,

$$\gamma_{II} = \left(-\frac{2D^2}{bh}\right)\left[\sqrt{1 - \left(\frac{D+d}{ct}\right)^2} - \ell n\left|\frac{1 + \sqrt{1 - \left(\frac{D+d}{ct}\right)^2}}{\frac{D+d}{ct}}\right|\right], \quad (56)$$

where $ct = ct_r + D$ and d is as defined in Equation 55.

For $\frac{b}{D} \le \frac{ct_r}{D} \le \sqrt{\left(1 + \frac{b}{D}\right)^2 + \left(\frac{h}{2D}\right)^2} - 1$,

$$\gamma_{II} = \left(-\frac{2D^2}{bh}\right)\left\{\sqrt{1 - \left(\frac{D+d}{ct}\right)^2} - \ell n\left|\frac{1 + \sqrt{1 - \left(\frac{D+d}{ct}\right)^2}}{\frac{D+d}{ct}}\right|\right.$$

$$\left. - \sqrt{1 - \left(\frac{D+b}{ct}\right)^2} + \ell n\left|\frac{1 + \sqrt{1 - \left(\frac{D+b}{ct}\right)^2}}{\frac{D+b}{ct}}\right|\right\}. \quad (57)$$

In the final time interval of interest, namely, $ct_r/D \ge \sqrt{(1 + b/D)^2 + (h/2D)^2} - 1$, the observer can "see" the entire source region and γ becomes the constant

$$\gamma = \gamma_F = \left(-\frac{2D^2}{bh}\right) \ell n\left|\left(\frac{1}{1 + \frac{b}{D}}\right)\left(\frac{\frac{h}{2D} + \sqrt{\left(1 + \frac{b}{D}\right)^2 + \left(\frac{h}{2D}\right)^2}}{\frac{h}{2D} + \sqrt{1 + \left(\frac{h}{2D}\right)^2}}\right)\right|. \quad (58)$$

Upon examining this rather confusing array of formulas, one can see that γ increases monotonically with time from a value of zero (when the observer first "sees" the source region) to a final constant value of γ_F (when the observer "sees" all of the source region). The parameter γ is plotted as a function of dimensionless retarded time (ct_r/D) in Figure 12 for the specific case of $b = h = D$. In this case, $\gamma_F = .467$.

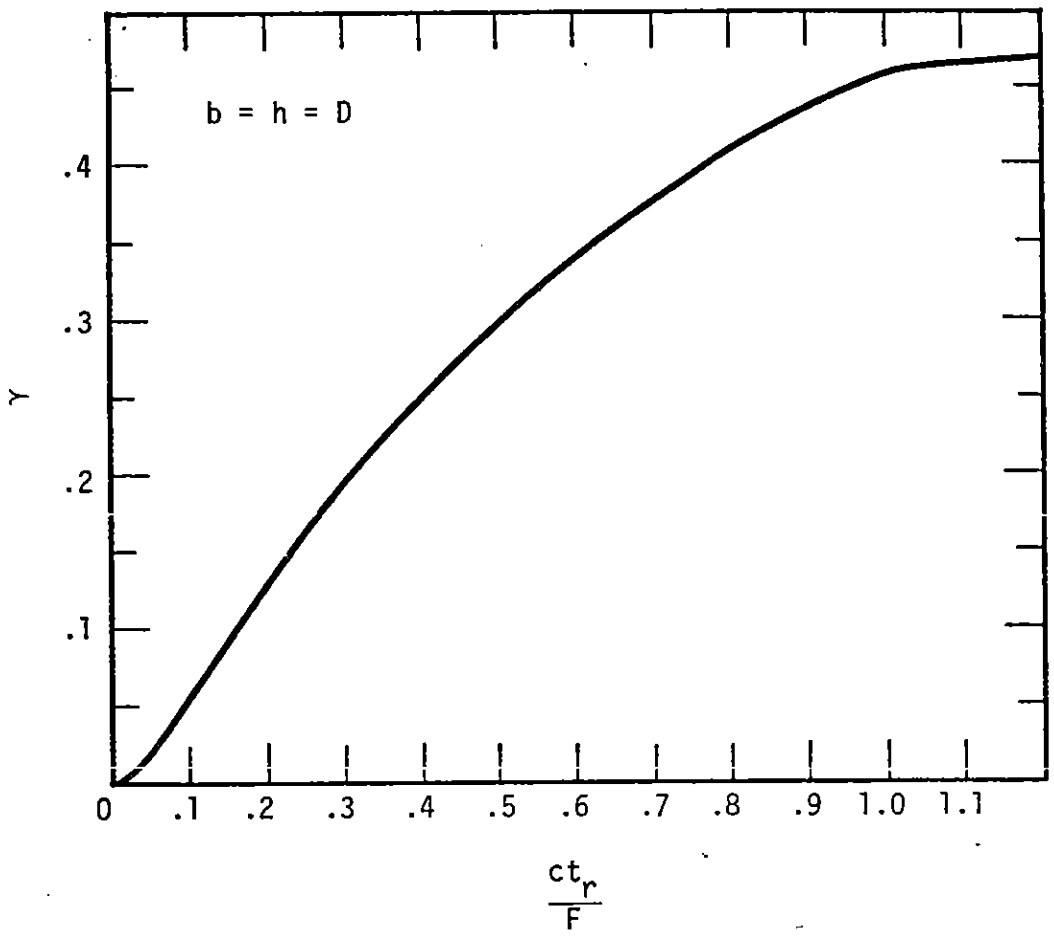

Figure 12. The parameter γ (see Equation 51) as a function of dimensionless retarded time for b = h = D.

The normalized magnetic field (from Equation 51) for this case is then plotted in Figure 13. This curve is just a plot of $(ct_r/D + 1)\gamma$. Note that the step-function discontinuities that were present for the point source (see Figure 2) are now missing because it takes some finite amount of time for the observer to "see" the source region.

Remember that it has been assumed that the current density is linearly rising. If the pulse is actually triangular and the risetime T_1 is sufficiently long for the observer to "see" the entire source region before the current density begins decreasing, the peak magnetic field is given by

$$H_{peak} = - \frac{a}{2\pi} \frac{(J_0 bh)}{D} \frac{\gamma_F}{cT_1} \left(\frac{cT_1}{D} + 1\right) . \qquad (59)$$

The peak replacement current densities will thus be similar to the point source case (see Equation 30 and corresponding discussion) but multiplied by γ_F, which is just a geometric term depending on the finite size of the source.

Note that Equations 46 and 58 indicate that for $D >> b,h$, $\gamma_F = 1$. A plot of γ_F as a function of D/b for various values of h/b is shown in Figure 14. It is obvious that the peak field from a finite source will be smaller than from a point source.

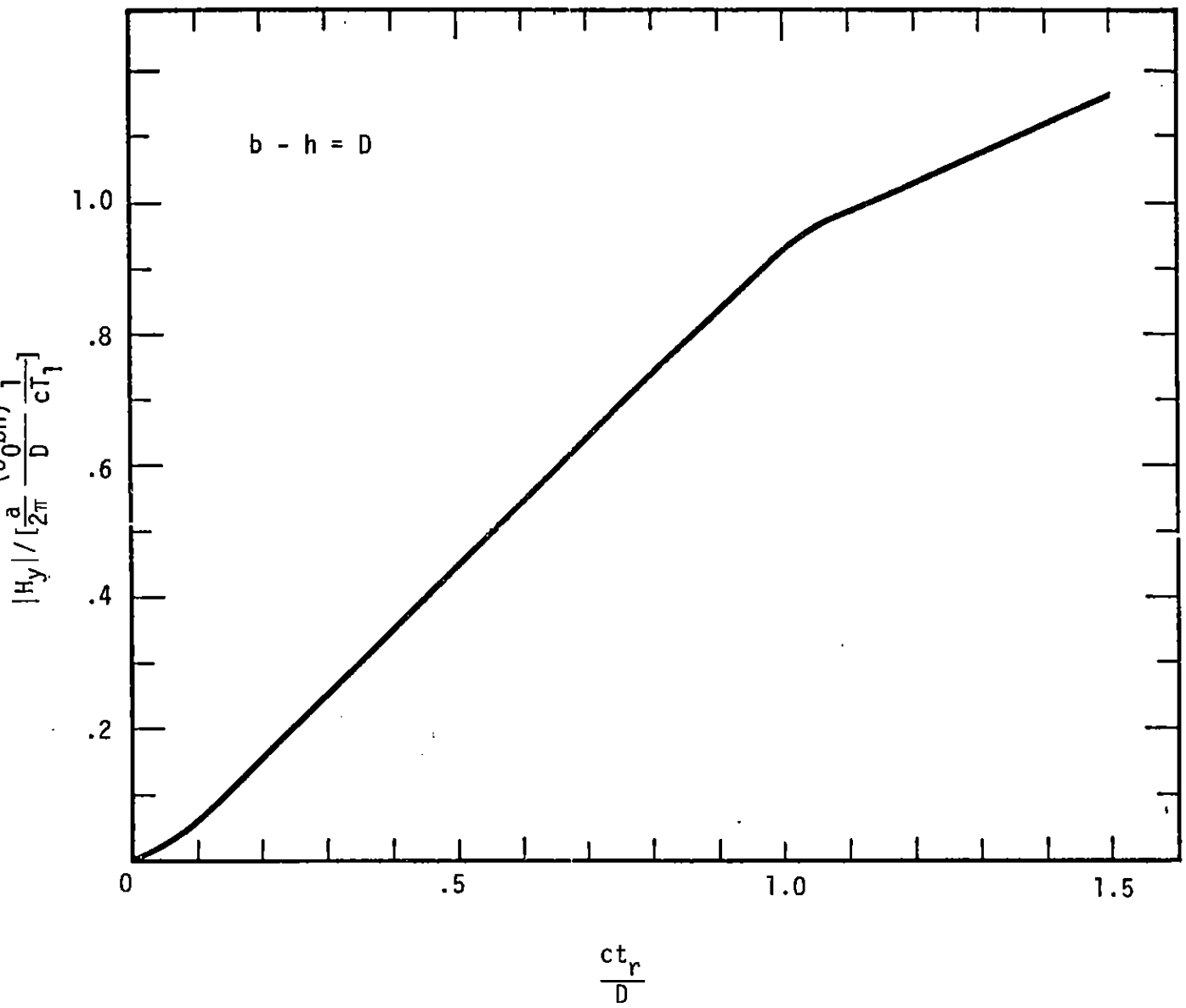

Figure 13. Normalized magnetic field for a rectangular source region with b = h = D.

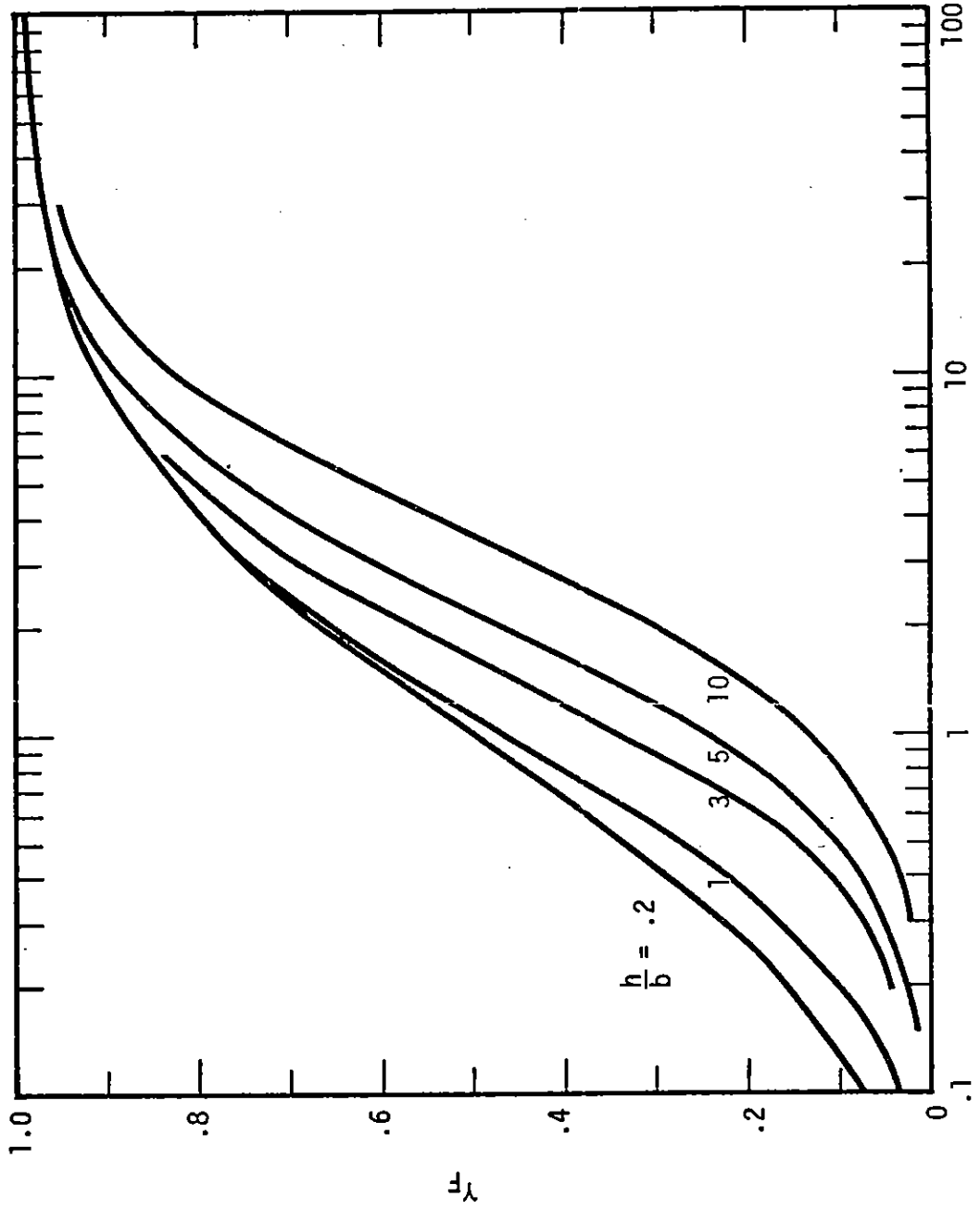

Figure 14. Y_F as a function of D/b for several values of h/b.

SECTION 5

RESULTS AND SUMMARY

This report began by writing down several different general expressions for the electromagnetic in free space that result from a specified source distribution. It was seen that both $\vec{E}$ and $\vec{H}$ can be written in terms of integrals containing the source charge density, ρ, and current density, $\vec{J}$.

These general expressions were then used in Section 3 to calculate the electromagnetic fields from a point dipole with several different current time histories. These specific expressions make it easy to identify the static, quasi-static, and radiation-zone parts of the electromagnetic fields. It was pointed out that waveform shapes range from monopolar to bipolar as the observer moves from the static region to the radiated field region. The parameter specifying these regions was seen to be cT/R, where c is the speed of light, T is the current pulse width (or rise time) and R is the distance to the observer. For large cT/R, the fields are quasi-static; for $cT/R \leq 1$, radiation terms are more important.

The magnetic field from a finite size source region with a linearly rising current time history was investigated in Section 4. It was shown that fields from a finite size source region will be smaller than from a point source emitting the same peak current.

The primary result of this work is a set of analytic expressions for the fields from a highly space-charge limited SGEMP boundary layer. It

is hoped that these expressions will be useful in increasing a general understanding of this phenomena and for comparison with detailed computer calculations. In the future, it may be useful to compare these results with the fields due to that part of the electron cloud that penetrates the boundary layer, since in some cases the boundary layer fields may be the dominant source of satellite response.

REFERENCES

1. Higgins, D. F., and C. L. Longmire, "Highly Space-Charge Limited SGEMP Calculations," Air Force Weapons Laboratory, Theoretical Note 277 (also MRC-R-190 and DNA 3885T), June 1975.

2. Carron, N. J., and C. L. Longmire, "On the Structure of the Steady-State, Space-Charge-Limited Boundary Layer in One Dimension," Air Force Weapons Laboratory, Theoretical Note 281 (also MRC-R-240 and DNA 3928T), November 1975.